Visual Abstract

Effect of composition and heat treatment on the mechanical properties of Fe Mn Al steels

A. Mondal, D. Pilone, A. Brotzu, F. Felli
DICMA, Sapienza Università di Roma, Via Eudossiana 18, 00184 Roma, Italy
avishek.mondal@uniroma1.it, https://orcid.org/0000-0001-6292-4418
daniela.pilone@uniroma1.it, https://orcid.org/0000-0002-8757-8360
andrea.brotzu@uniroma1.it, https://orcid.org/0000-0001-9530-4602
ferdinando.felli@uniroma1.it, https://orcid.org/0000-0002-7527-8096

ABSTRACT. Starting from the research aimed at the development of substitute alloys for stainless steels, with the aim of replacing strategic metals such as chromium and nickel with the more available manganese, FeMnAlC alloys have been studied and developed for several years. These alloys exhibit an attractive strength/ductility combination, low density, and some of them show good oxidation behaviour at high temperatures. In this work we studied alloys with novel compositions to highlight the effect of heat treatments on their mechanical behaviour, in order to tailor alloy composition and process parameters for a specific application. After a preliminary study, in this paper the effect of a solubilization treatment followed by aging in the temperature range 550 - 750 °C has been evaluated. The results of the investigation revealed that the steel characterized by the higher amount of Mn and Al shows, after heat treatment, the formation of phases that make the alloy very brittle. Considering the obtained results, it is evident that optimizing the alloy chemical composition is of paramount importance to guarantee a high fracture toughness if the steel works for limited time intervals at high temperature.

KEYWORDS. Aging treatment; FeMnAl steels; Low density steels; Mechanical properties.

OPEN ACCESS

INTRODUCTION

Owing to an attractive combination of strength and ductility Fe-Mn-Al-C alloys have been intensively studied since the last 70 years. Due to their potential applications for structural components in the automotive [1] and cryogenic industries, these steels were developed to replace conventional Fe-Ni-Cr steels in the 1950s. In addition to these,

Fe-Mn-Al-C alloys are also used in aircraft and chemical industry because of their good oxidation resistance at high temperatures and corrosion resistance, but with a specific composition for each application.

According to available research, it should be highlighted that the addition of Al to Fe-C steels leads to a reduction in both density and Young's modulus. A 1 wt.% of aluminium addition results in about 1.3% decrease in density [2] , which is an important achievement for reducing fuel consumption and CO_2 emissions for the automotive sector. Lightweight Fe-Mn-Al-C alloys can be classified into different categories, but among them, twinning-induced plasticity (TWIP) steels with up to 30 wt.% Mn and > 0.4 wt.% C content have shown a promising combination of ductility and strength.

When Mn is added to Fe-Al-C steels, it increases the face-centered lattice parameter. Moreover, high Mn and C content stabilizes the austenite, so that it can tolerate Al addition up to about 10 wt.% without destabilizing the FCC structure [3,4,5]. It has been found that 1% Al addition causes a reduction of 2-2.5% of Young's modulus, due to the reduction of lattice energy of the Fe-Al solid solution and the greater distance between Fe and Al atoms in the lattice [6]. Similarly, Mn addition decreases the Young's modulus of the alloy [7].

In terms of microstructure, Fe-Mn-Al-C lightweight alloys are generally characterized by the presence of five main phases: α – ferrite, austenite, k-carbides, M_xC_y carbides and β-Manganese[8]. The ferritic alloy is formed when the alloy contains a low Mn content (< 5 wt.%), 5-9 wt.% Al and a low C content (< 0.1 wt.%) [9]. The research available in the literature concerns steels having a high Mn content (15- 38 wt.%), an Al content of 2-12 wt.%, and a high C content (0.5-2.0 wt.%), which intrinsically tends to form austenitic Fe-Mn-Al-C steels [9].

Austenite plays an essential role in these types of steels, not because of the excellent mechanical properties but because of its possible various microstructural evolutions. To produce these austenite based low density steels, there are various process available. The two main processes are cold rolling and hot rolling. In our research, the steels that are studied are manufactured by cold rolling. To obtain cold rolled Fe-Mn-Al-C steels with age-hardenable austenitic structure, the cold rolled strips are solution treated over a temperature range of 900-1100 °C in the single austenite phase area, and then quenched. Subsequently, aging treatments can be performed to produce precipitation hardening, that is carried out by isothermally holding the material at a temperature varying over the range of 500-700 °C [10,11,12]. For non-age hardenable austenitic Fe-Mn-Al-C steels, after cold rolling, they can be briefly annealed in the temperature range of 600-900 °C to restore ductility.

Because of the high reachable strength of these alloys, many studies have been performed on the strengthening mechanisms. Regarding the strengthening mechanism of these steels, the available literature highlights that austenitic low-density steels can be strengthened by means of solution hardening, work hardening, grain refinement [13] and precipitation hardening. While grain refinement is generally applied for non-age hardenable Fe-Mn-Al-C alloys, precipitation hardening is a very significant strengthening mechanism for highly alloyed Fe-Mn-Al-C alloys. This mechanism determines the formation of nanoscale and homogeneously distributed k^I-carbides, which influence the movement and arrangement of dislocations during deformation [14,15,16].

In addition to cryogenic applications, these alloys are also studied for applications at high temperatures. Some authors reported that, by increasing the aluminium content above 7%, it was possible to decrease the oxidation rate due to the formation of a layer of $FeAl_2O_4$ and Al_2O_3 [17,18] . While to increase the oxidation resistance, 2.3% Si can be added [19]. Other authors [20,21,22] emphasized that steel behaviour is closely related to the alloy composition. For example, Fe- (5-10) % Mn- (6-10)% Al alloys develop continuous protective alumina scales over the temperature range 600-1000 °C and are completely ferritic. Austenite appears to be detrimental to the oxidation resistance of duplex alloys as it promotes the degradation of the aluminium oxide layer and the growth of Mn-rich oxides.

In this work, after a preliminary study [23], four Fe-Mn-Al-C alloys with potentially interesting applications, were investigated to evaluate the influence of heat treatments on their mechanical and fracture behaviour. The manganese and aluminium content of the alloy determines its mechanical properties and its behaviour during thermal treatment.

EXPERIMENTAL

For this research, four kinds of rolled steels having a thickness of 5 mm were considered. The compositions of the four considered alloys are reported in Tab. 1.

The alloys having a composition varying over the following ranges (wt.%) have been considered: 0.76- 0.96% C, 26-37% Mn, 6-10% Al. One of the considered alloys (B22) also contains 1.25% Si. In the as-received conditions, all alloys are characterized by an austenitic structure. Only the alloys containing a lower percentage of Mn and a higher percentage of Al and the one containing Si show the presence of a low percentage of ferrite.

	C	Mn	Al	Si	Fe
B22	0.96	30.8	6.5	1.25	bal.-
B23	0.76	37.2	9.5	0.0	bal.-
B37	0.96	32.8	5.6	0.0	bal.-
B41	0.95	26.3	6.0	0.0	bal.-

Table 1: Chemical composition (wt %) of the four specimens.

To perform the tests, the steels were cut into appropriate sizes to perform the aging and tensile tests. For each type of steel and test conditions three specimens were used to validate the results. Furthermore, specimens with a size of 25 x 25 x 5 mm were cut and ground using SiC papers ranging from 80 to 2400 grit and then polished using 1µm colloidal alumina suspension to perform metallographic analyses. To reveal the microstructure, they were etched using freshly prepared Nital 5 solution for a time ranging from 10 seconds to 45 seconds.

The aging tests were performed by performing a solution treatment at 1030 °C for 60 minutes and 1050 °C for 30 minutes, quenching in water and aging at 550-700 °C for different times. Specimen hardness was also measured at regular intervals in order to obtain specimen hardness as a function of treatment time.

Tensile tests were performed on as-received specimens and on specimens after aging at 550°C by using an Instron 3367 machine.

To identify the phases before and after heat treatment, X-ray diffractions were performed using a Philips X'pert diffractometer using a Cu(Kα) source. The test conditions were set to be: accelerating voltage 40 kV, current 40 mA, scan step 0.02 degrees, scan step time 2 s. Fracture surfaces and microstructures were analyzed by using a Hitachi scanning electron microscope (SEM) equipped with energy dispersion spectroscopy (EDS).

RESULTS AND DISCUSSION

The analysis of steels started with the study of their microstructure. The four types of steel specimens were analyzed by using an optical microscope. Fig. 1 shows the microstructure of the four alloys in the as-received state. Fig. 1 highlights that all alloys have a typical austenitic structure with visible twins. From the microstructure it is evident that the average grain size of the austenite grain ranges from 50 to 200 µm.

By observing the microstructure, it can be noticed that all four specimens have an austenitic structure before heat treatment. Moreover, to characterize the as-received alloys, material density measurements were performed using Archimedes' method. The overall density (Tab. 2) ranged between 6.5 and 7.2 g/cm³. Vickers hardness tests were conducted on the as-received specimens. All four alloys showed a hardness ranging from 175 HV10 to 221 HV10.

Fig. 2 shows the aging curves of the studied alloys at different temperatures. This figure highlights that, by varying the temperature and time of solubilization and by varying the aging temperature over the range 550-700 °C, differences among the aging curves can be observed. While the hardness of B23 and B22 specimens increases with time, the hardness of the other specimens remains almost constant or only shows a small increase. In Fig. 2, the blue curves show the behavior of specimens subjected to solubilization at 1030°C for 1 hour before aging, while the red curves represent the behavior of specimens subjected to solubilization of the alloy at 1050°C for 30 minutes before aging. This behaviour cannot be easily explained, but it can be highlighted that the alloys characterized by higher amounts of Al and Mn show a higher tendency to harden during thermal treatment. According to the literature [24,1], the decrease in ductility and toughness of Fe-Mn-Al-C alloys after solubilization, quenching and aging at around 550 °C is due to the formation of k-carbides which tend to precipitate along the austenite grain boundaries and within the austenite matrix. Depending upon the amount of alloying elements, k-carbides, α-ferrite and β-Mn phases may be formed and produce a hardness increase of the alloy. By observing Fig. 2, it is possible to see that alloys solubilized for shorter times increase their hardness for shorter heat treatment times. This could be due to the incomplete solubilization of alloying elements that could produce the formation of nuclei for the precipitation of hardening phases. As it can be observed in Fig. 2, by increasing the heat treatment time, the red and blue lines tend to converge toward similar values. Specimens subjected to solubilization and aging for 8 hours along with specimens in the as-received conditions were subjected to tensile tests. The tests were carried out according to ASTM E8M standards [25]. Fig. 3 shows the stress-strain curves of an alloy (B23) that hardens after heat treatment and the stress-strain

curves of an alloy (B37) that doesn't harden after heat treatment. These curves describe two different behaviours after aging. The alloy mechanical behaviour is shown in the as-received conditions and after heat treatment.
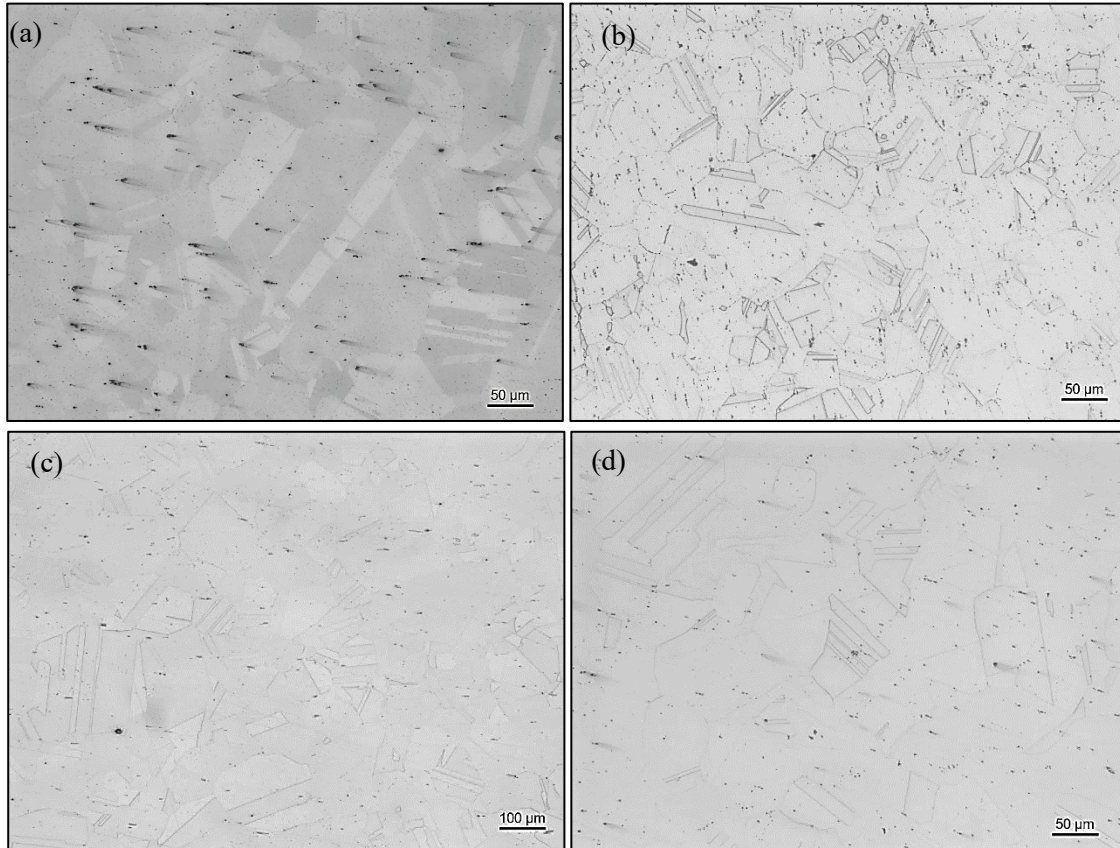

Figure 1: Microstructure of (a) B22, (b) B23, (c) B37 and (d) B41 in as-received state.

	Density (g/cm³)	Hardness (HV10)
B22	6.8	221±5
B23	6.5	209±5
B37	7.1	175±6
B41	7.2	182±7

Table 2: Density and hardness of the four specimens in the as-received conditions.

As it can be seen in Fig. 3, B23 showed a very brittle behaviour after 8 hours of aging at 550 °C and broke in the elastic region. For B23 in the as-received conditions, the yield strength is 450 MPa with a tensile strength of 727 MPa and an elongation of 21%. For B37, the yield strength is about 402 MPa with a maximum tensile strength of 801 MPa and elongation of 30%. Tensile tests performed after heat treatment showed that B37 has a mechanical behaviour very similar to the one exhibited in the as-received conditions: the yield strength was 422 MPa with a tensile strength of 817 MPa and an elongation of 37.6%.

To study the different behaviour shown by the different alloys, a microstructural analysis has been performed after heat treatment. Fig. 4 shows the microstructure of all the alloys after 8-hour aging. It can be seen that while B37 and B41 have the typical austenitic structure as before the heat treatment, the microstructure of B23 has completely changed and appears to be characterized by the presence of different phases. B22 specimen still has an austenitic structure, but grains have a quite different morphology: they appear more rounded. It must also be stressed that, after aging, B23 shows the presence of delamination defects that can affect the mechanical behaviour of the alloy.
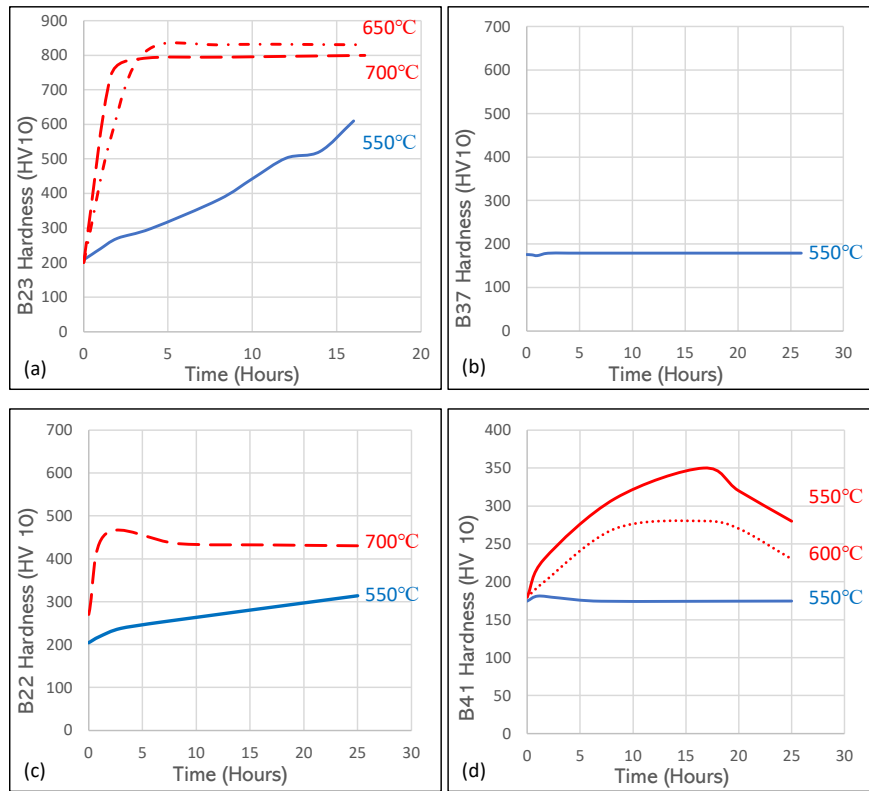
Figure 2: Aging curves of (a) B23, (b) B37, (c) B22 and (d) B41 at different temperatures. The red lines show the behaviour of specimens solubilized at 1050 °C for 0.5 h, while the blue lines show the behaviour of specimens solubilized at 1030 °C for 1 hour.
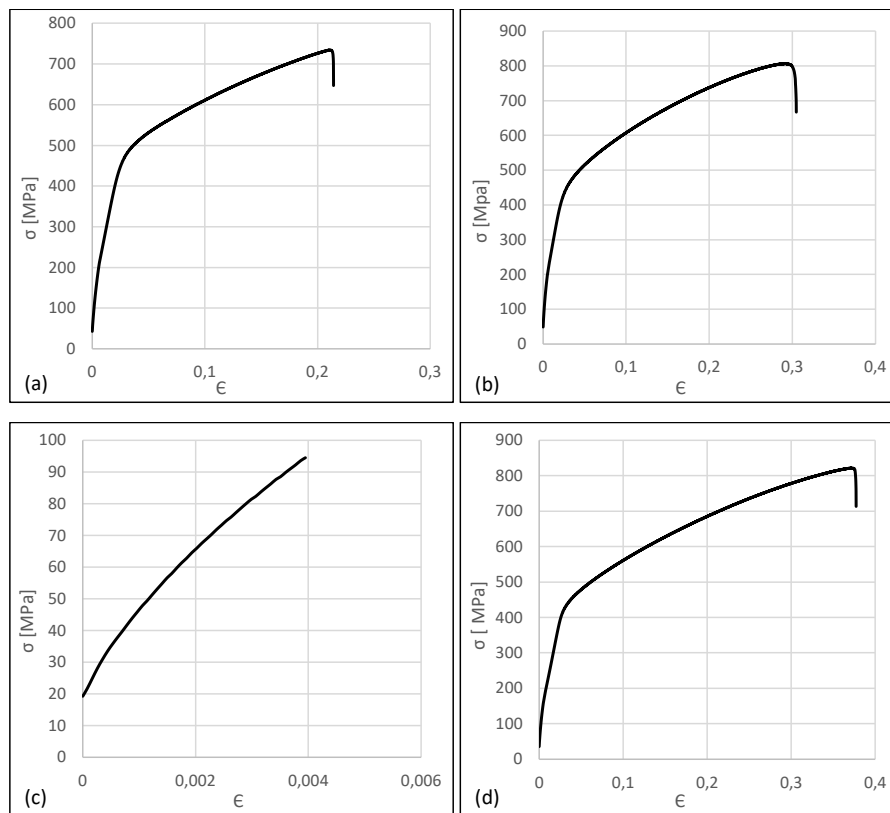

Figure 3: Stress-strain curves of (a) B23 and (b) B37 in the as-received conditions. Stress-strain curves of (c) B23 and (d) B37 after heat treatment at 550 °C for 8 hours.
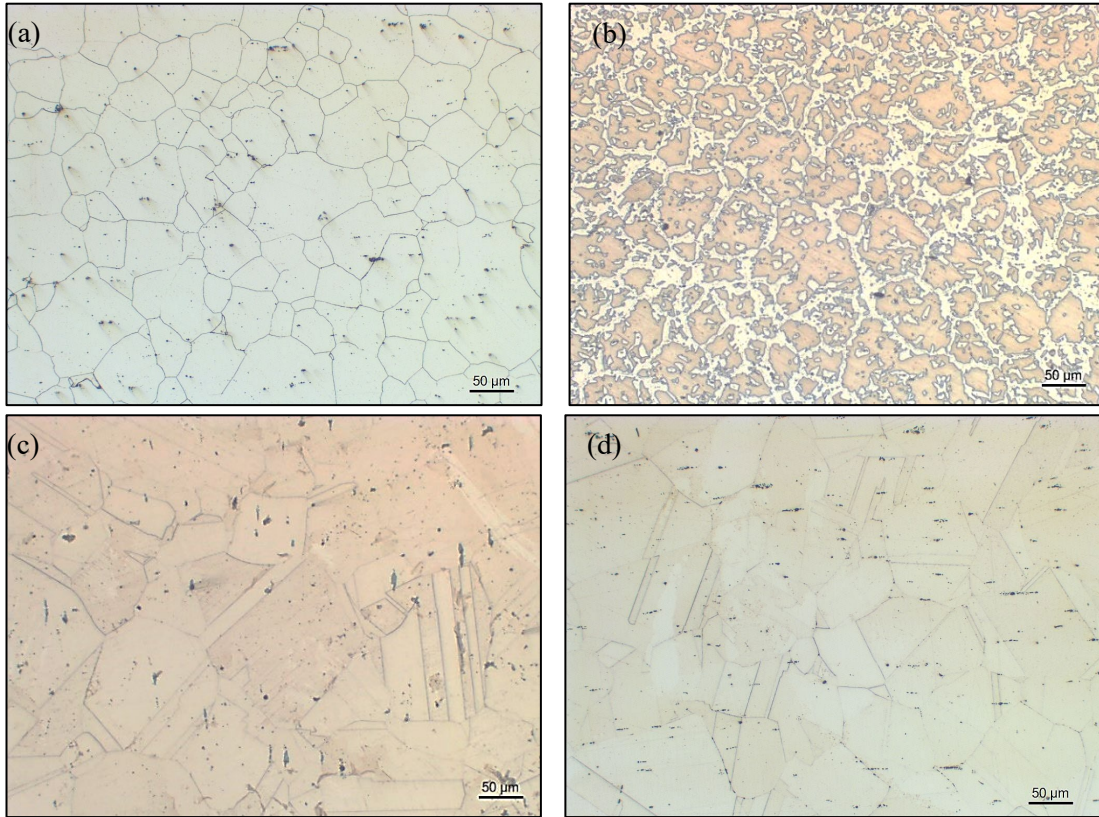
Figure 4: Microstructure after solution treatment and aging (a) of B22, (b) of B23, (c) of B37 and (d) of B41.

To understand the behaviour of B22 specimen, which hardened after heat treatment, the alloy structure was also analysed by SEM. Fig. 5 shows the SEM micrographs of the alloy that reveal that there is an intergranular precipitation of carbides that harden the alloy.
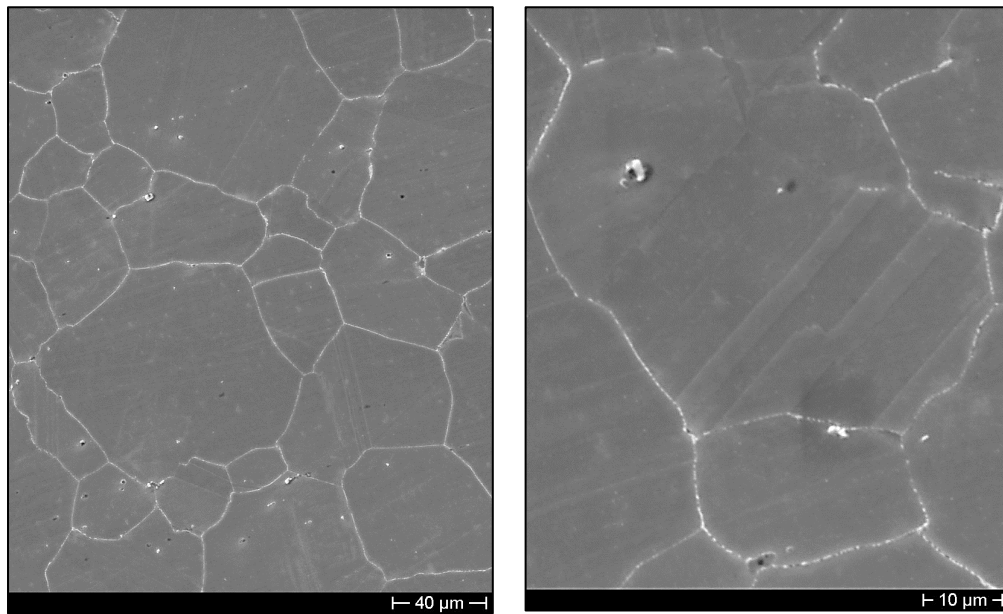

Figure 5: SEM micrographs showing the microstructure of B22, at different magnifications, after 8 hours of aging.

As far as the B23 specimen is concerned, to explain the causes of the brittle behaviour of this alloy after heat treatment, XRD analyses have been performed on the specimens in the as-received state and in the aged conditions.

As it can be observed in Fig. 6, before heat treatment, the alloy is constituted by austenite and by a little amount of ferrite. After heat treatment (Fig. 7), intermetallic phases, such as Al8Mn5, FeMn4 and FeMn3, are formed. This explains the change in the microstructure and the alloy brittle behaviour during the tensile test. The fracture of the alloy in the elastic region is justified by the presence of intermetallic phases, which are very brittle, and by the presence of delamination defects that act as stress intensifiers.
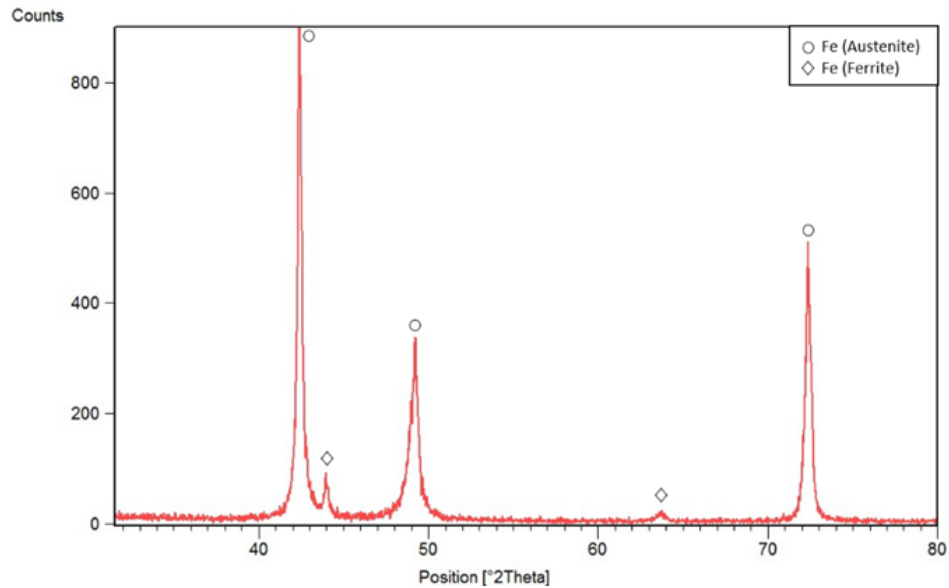

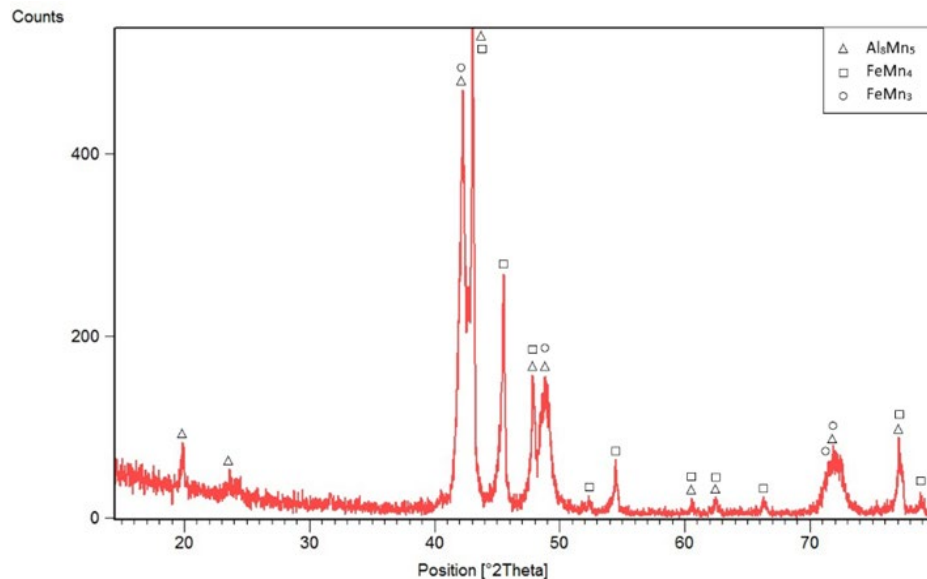Figure 6: XRD diffraction patterns of B23 before heat treatment.

Figure 7: XRD diffraction patterns of B23 after heat treatment.

To understand the fracture behaviour of the alloys studied, the fracture surfaces of all steels were analyzed by means of SEM. Figs. 8 (a) and (c) show the fracture surfaces of B23 and B37 obtained from the tensile test before heat treatment. Before heat treatment, both steels have similar fracture surface morphology, characterized by dimples, which are ductile in nature. After tensile tests, both specimens developed delamination layers whose presence can be attributed to the hot rolling performed in the production stage.

Figs. 8 (b) and (d) show the fracture surfaces of B23 and B37 after heat treatment. By observing this figure, it is evident that B37 shows a ductile fracture, similar to the one observed before heat treatment. Quite the opposite, B23 shows a brittle behaviour with a transgranular fracture characterized by the presence of secondary microcracks (Fig. 8(b)). In fact, as shown

by XRD pattern in Fig. 7, heat treatment of B23 determined the formation of brittle intermetallic phases through which microcracks formed during the test, can easily propagate in an instable manner.
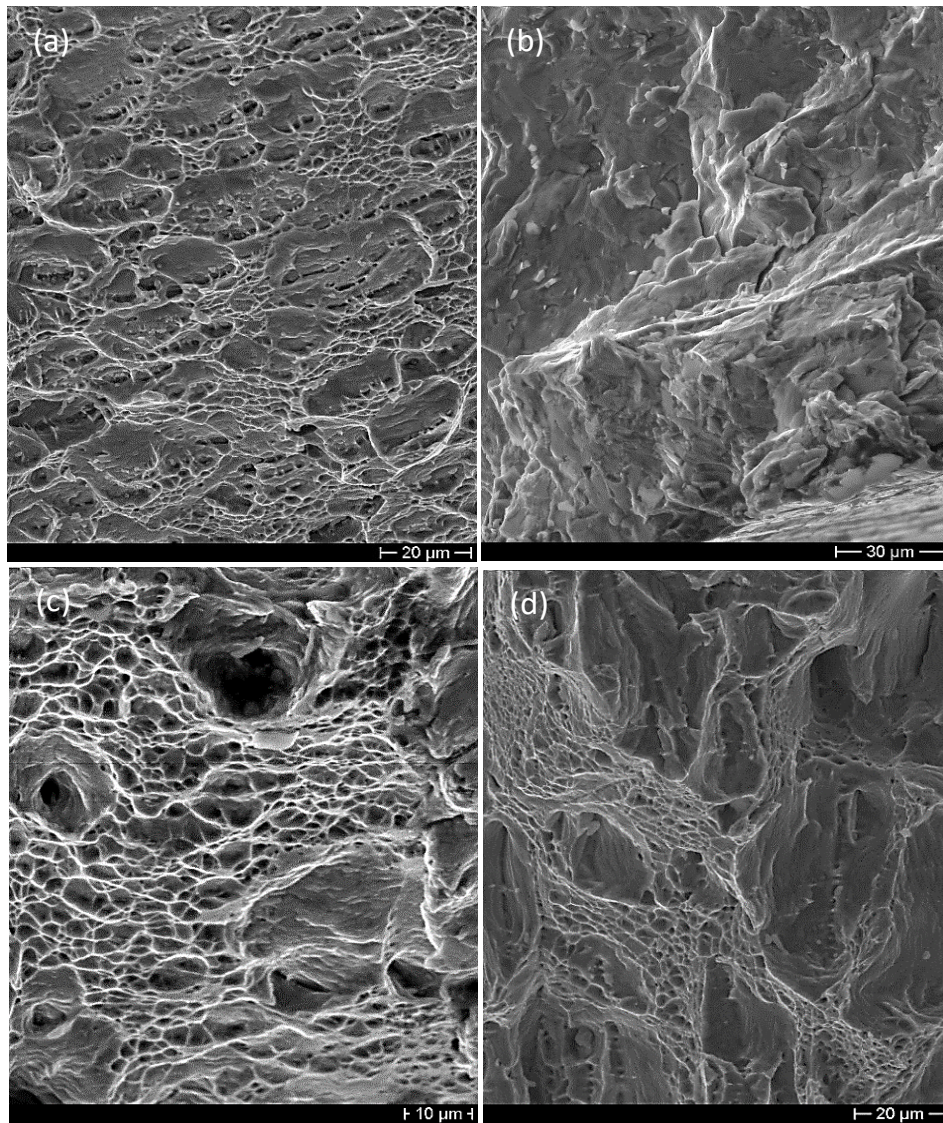

Figure 8: SEM micrographs showing the fracture surface morphologies of sample B23 before (a) and after (b) heat treatment and of sample B37 before (c) and after (d) heat treatment.

CONCLUSIONS

From this research it is evident that the composition of the studied steels affects their behaviour, especially when they work at a temperature above the range 500-700 °C. Microstructural analyses carried out on the four different considered alloys showed that they were characterized by an austenitic structure in the as-received state, but solution treatment and aging had different effect on their microstructure and mechanical properties. The alloy characterized by the highest content of Mn and Al, after heat treatment, produced the formation of brittle intermetallic phases that determined a brittle behavior of the alloy. By studying the effect of heat treatment on the other studied alloys, it has been observed that, depending on the alloy composition, aging heat treatments can significantly raise the alloy hardness by decreasing the alloy fracture toughness, as it is evident from tensile tests. On the basis of this observation, it is not advisable to perform heat treatments to raise the mechanical properties of these alloys if intermetallic phases can form. It must also be considered that the studied alloys show interesting mechanical properties also in the as-received conditions.

Moreover, for FeMnAlC alloys, optimizing the chemical composition is of paramount importance to guarantee a high ductility and fracture toughness when the component is put in service at high temperature.

REFERENCES

[1] Chen, S., Rana, R., Haldar, A., Ray, R.K. (2017). Current state of Fe-Mn-Al-C low density steels, Prog. Mater Sci., 89, pp. 345–391. DOI: 10.1016/j.pmatsci.2017.05.002.

[2] Frommeyer, G., Brüx, U. (2006). Microstructures and mechanical properties of high-strength Fe-Mn-Al-C light-weight TRIPLEX steels, Steel Res. Int., 77(9–10), pp. 627–633. DOI: 10.1002/srin.200606440.

[3] Ishida, K., Ohtani, H., Satoh, N., Kainuma, R., Nishizawa, T. (1990). Phase Equilibria in Fe-Mn-AI-C Alloys, ISIJ Int., 30(8), pp. 680–686. DOI: 10.2355/isijinternational.30.680.

[4] Kalashnikov, I., Acselrad, O., Shalkevich, A., Pereira, L.C. (2000). Chemical composition optimization for austenitic steels of the Fe-Mn-Al-C system, J. Mater. Eng. Perfor., 9(6), pp. 597–602. DOI: 10.1361/105994900770345430.

[5] Raabe, D., Springer, H., Gutierrez-Urrutia, I., Roters, F., Bausch, M., Seol, J.B., Koyama, M., Choi, P.P., Tsuzaki, K. (2014). Alloy Design, Combinatorial Synthesis, and Microstructure–Property Relations for Low-Density Fe-Mn-Al-C Austenitic Steels, JOM, 66(9), pp. 1845–1856. DOI: 10.1007/s11837-014-1032-x.

[6] Lehnhoff, G.R., Findley, K.O., de Cooman, B.C. (2014). The influence of silicon and aluminum alloying on the lattice parameter and stacking fault energy of austenitic steel, Scr. Mater., 92, pp. 19–22. DOI: 10.1016/j.scriptamat.2014.07.019.

[7] Bohnenkamp, U., Sandström, R. (2000). Evaluation of the elastic modulus of steels, Steel Res., 71(3), pp. 94–99. DOI: 10.1002/srin.200005696.

[8] Mapelli, C., Barella, S., Gruttadauria, A., Mombelli, D., Bizzozero, M., Veys, X. (2020). γ Decomposition in Fe–Mn–Al–C lightweight steels, J. Mater. Res. Technol., 9(3), pp. 4604–4616. DOI: 10.1016/j.jmrt.2020.02.088.

[9] Gutierrez-Urrutia, I. (2021). Low density Fe-Mn-Al-C Steels: Phase structures, mechanisms and properties, ISIJ Int., 61(1), pp. 16–25. DOI: 10.2355/isijinternational.ISIJINT-2020-467.

[10] Gutierrez-Urrutia, I., Raabe, D. (2013). Influence of Al content and precipitation state on the mechanical behavior of austenitic high-Mn low-density steels, Scr. Mater., 68(6), pp. 343–347. DOI: 10.1016/j.scriptamat.2012.08.038.

[11] Kim, H., Suh, D.W., Kim, N.J. (2013). Fe-Al-Mn-C lightweight structural alloys: A review on the microstructures and mechanical properties, Sci. Technol. Adv. Mater., 14(1). DOI: 10.1088/1468-6996/14/1/014205.

[12] Rana, R. (2014). Low-Density Steels, JOM, 66(9), pp. 1730–1733. DOI: 10.1007/s11837-014-1137-2.

[13] Etienne, A., Massardier-Jourdan, V., Cazottes, S., Garat, X., Soler, M., Zuazo, I., Kleber, X. (2014). Ferrite effects in Fe-Mn-Al-C triplex steels, Metall. Mater. Trans. A, 45(1), pp. 324–334. DOI: 10.1007/s11661-013-1990-6.

[14] Ikarashi, Y., Sato, K., Yamazaki, T., Inoue, Y., Yamanaka, M. (1992). Age-hardening and formation of modulated structures in austenitic Fe-Mn-AI-C alloys, J. Mater. Sci. Lett., 11, pp. 733-735. DOI: 10.1007/BF00729475.

[15] Park, S.W., Park, J.Y., Cho, K.M., Jang, J.H., Park, S.J., Moon, J., Lee, T.H., Shin, J.H. (2019). Effect of Mn and C on Age Hardening of Fe–Mn–Al–C Lightweight Steels, Met. Mater. Int., 25(3), pp. 683–696. DOI: 10.1007/s12540-018-00230-x.

[16] Song, W., Zhang, W., von Appen, J., Dronskowski, R., Bleck, W. (2015). ϰ-phase formation in Fe-Mn-Al-C austenitic steels, Steel Res. Int., 86(10), pp. 1161–1169. DOI: 10.1002/srin.201400587.

[17] Kao, C.H., Wan, C.M. (1988). Effect of manganese on the oxidation of Fe-Mn-Al-C alloys, J. Mater. Sci., 23(2), pp. 744–752. DOI: 10.1007/BF01174715.

[18] Zambrano, O.A. (2018). A general perspective of Fe–Mn–Al–C steels, J. Mater. Sci., 53(20), pp. 14003–14062. DOI: 10.1007/s10853-018-2551-6.

[19] Felli, F., Bernabai, U., Cavallini, M. (1985). Influence of silicon on oxidation behaviour of Fe-Mn-Al and Fe-Mn alloys. Metall. Sci. Technol., 3, pp. 87-94.

[20] Jackson, P.R.S., Wallwork, G.R. (1984). High temperature oxidation of iron-manganese-aluminum based alloys, Oxid. Met., 21(3–4), pp. 135–170. DOI: 10.1007/BF00741468.

[21] Sauer, J.P., Rapp, R.A., Hirth, J.P. (1982). Oxidation of iron-manganese-aluminum alloys at 850 and 1000°C, Oxid. Met., 18(5–6), pp. 285–294. DOI: 10.1007/BF00656572.

[22] Pérez, P., Pérez, F.J., Gómez, C., Adeva, P. (2002). Oxidation behaviour of an austenitic Fe–30Mn–5Al–0.5C alloy. Corr. Sci., 44(1), pp. 113-127. DOI: 10.1016/S0010-938X(01)00043-9.

[23] Mondal, A., Pilone, D., Brotzu, A., Felli, F. (2021). Effect of heat treatment on mechanical properties of FeMnAlC alloys, Procedia Struct. Integrity, 33, pp. 237–244. DOI: 10.1016/j.prostr.2021.10.029.

[24] Benz, J.C., Leavenworth, H.W. (1985). An Assessment of Fe-Mn-Al Alloys as Substitutes for Stainless Steels, JOM, 37(3), pp. 36–39. DOI: 10.1007/BF03258661.

[25] ASTM E8 / E8M-21, Standard Test Methods for Tension Testing of Metallic Materials, ASTM International, West Conshohocken, PA, 2021, www.astm.org, DOI: 10.1520/E0008_E0008M-21.